
Improving IRMPD in a Quadrupole Ion Trap

G. Asher Newsome and Gary L. Glish

Department of Chemistry, University of North Carolina at Chapel Hill, Chapel Hill, North Carolina, USA

A focused laser is used to make infrared multiphoton photodissociation (IRMPD) more efficient in a quadrupole ion trap mass spectrometer. Efficient (up to 100%) dissociation at the standard operating pressure of 1×10^{-3} Torr can be achieved without any supplemental ion activation and with shorter irradiation times. The axial amplitudes of trapped ion clouds are measured using laser tomography. Laser flux on the ion cloud is increased six times by focusing the laser so that the beam waist approximates the ion cloud size. Unmodified peptide ions from 200 Da to 3 kDa are completely dissociated in 2.5–10 ms at a bath gas pressure of 3.3×10^{-4} Torr and in 3–25 ms at 1.0×10^{-3} Torr. Sequential dissociation of product ions is increased by focusing the laser and by operating at an increased bath gas pressure to minimize the size of the ion cloud. (J Am Soc Mass Spectrom 2009, 20, 1127–1131) © 2009 Published by Elsevier Inc. on behalf of American Society for Mass Spectrometry

Infrared multiphoton photodissociation (IRMPD) has been used for tandem mass spectrometry in a quadrupole ion trap mass spectrometer [1–7] and a Fourier transform ion cyclotron resonance mass spectrometer [8–11] as an alternative to collision-induced dissociation (CID). Only one *m/z* ion is selected for excitation in conventional CID, limiting sequential dissociation of product ions into smaller mass product ions. Conversely, in IRMPD all parent and product ions are irradiated simultaneously with a collimated, IR laser providing the capability to generate abundant small mass product ions. IRMPD is typically performed in a quadrupole ion trap mass spectrometer at a smaller low mass cut-off (LMCO) than CID, allowing the observation of a broader *m/z* range of product ions [2, 4], and a higher MS/MS efficiency,

$$E_{\text{MS/MS}} = \frac{\sum_i F_i}{P_0} \times 100\%$$

where $E_{\text{MS/MS}}$ is MS/MS efficiency, F_i is the abundance of each product ion, and P_0 is the initial abundance of the parent ion before irradiation. IRMPD is performed in a Fourier transform ion cyclotron resonance mass spectrometer to eliminate the need for a CID target gas to be leaked into and pumped out of the ICR cell [10, 11].

The sensitivity of a quadrupole ion trap mass spectrometer is optimized with a bath gas pressure around 1.0×10^{-3} Torr. Bath gas collisions reduce the kinetic energy of trapped ions and minimize the size of the ion cloud [12]. However, collisions also remove internal energy gained from IR absorption, necessitating longer

periods of irradiation for dissociation and decreasing fragmentation efficiency [13],

$$E_F = \frac{\sum_i F_i}{\sum_i F_i + P} \times 100\%$$

where E_F is fragmentation efficiency, F_i is the abundance of each product ion, and P is the abundance of the parent ion remaining after irradiation. IRMPD in a quadrupole ion trap mass spectrometer often is performed at 1×10^{-5} to 3×10^{-4} Torr to decrease collisional cooling of parent ion internal energy [2–7], [13] and achieve dissociation with shorter irradiation times. However, this reduced bath gas pressure is less effective for trapping ions during injection and reduces sensitivity.

Several methods have been developed to increase IRMPD fragmentation efficiency by combining IRMPD with another form of ion activation and/or decreasing collisional cooling. Ions have been dissociated in a quadrupole ion trap mass spectrometer at 1×10^{-3} Torr with irradiation times comparable to IRMPD at lower pressures by using thermal assistance [4] or collisional activation before irradiation [14]. Pulsed introduction of the bath gas has also been used to increase trapping efficiency during ion injection, and then the gas is pumped away before irradiation [15]. Covalent attachment of IR-active ligands to increase the rate of absorption has been used to achieve dissociation in shorter irradiation times [16, 17]. The first example of IRMPD in a quadrupole ion trap mass spectrometer used a multi-pass optical system to increase the path length of the laser and overlap with the ion cloud [1]. In Fourier transform ion cyclotron resonance mass spectrometers collisional cooling is not an issue, but because of the large magnetron radius of the ions the laser is commonly left unfocused to maximize laser overlap [18];

Address reprint requests to Professor G. L. Glish, Department of Chemistry, University of North Carolina at Chapel Hill, Chapel Hill, NC 27599-3290, USA. E-mail: glish@unc.edu

irradiation times are commonly up to one order of magnitude longer than for IRMPD in a quadrupole ion trap mass spectrometer. The work reported here shows that focusing the laser for IRMPD in a quadrupole ion trap mass spectrometer is the most simple and effective means of increasing fragmentation efficiency. Peptide ions are shown here to be completely dissociated in as little as 3 ms by focusing the laser on the trapped ion cloud at 1.0×10^{-3} Torr, at least an order of magnitude shorter than irradiation times previously reported with a quadrupole ion trap mass spectrometer at any bath gas pressure.

Experimental

All experiments were performed on a modified Finnigan ITMS controlled with ICMS software [19]. Peptides were obtained from Sigma Chemical Co. and used without further purification. Samples were prepared as 25 μM solutions in 75:20:5 methanol:water:acetic acid. Base pressure in the quadrupole ion trap mass spectrometer without added bath gas was 2×10^{-5} Torr. Helium bath gas was added for a constant pressure of 3×10^{-4} Torr to 1×10^{-3} Torr. (Measurements were made at 3×10^{-4} Torr because this is the pressure just below where significant collisional cooling starts to occur [4].) There are no conductance limits in the electrode assembly so the pressure measured in the vacuum system is the pressure in the quadrupole ion trap mass spectrometer. A nano-electrospray source was used to generate parent ions: $[\text{PD} + \text{H}]^+$ (231 Da, m/z 231); $[\text{ALILTLVS} + \text{H}]^+$ (830 Da, m/z 830); $[\text{bradykinin} + 2\text{H}]^{2+}$ (1062 Da, m/z 531); and $[\text{melittin} + 4\text{H}]^{4+}$ (2850 Da, m/z 712). All parent ions were trapped at a q_z of 0.10.

A Synrad 50 W CO₂ laser triggered by a TTL pulse from the ITMS electronics is used for IRMPD. The laser beam is passed into the vacuum housing through a ZnSe window by optical elements mounted on translation stages. A ZnSe lens with a focal length of 38.1 cm can be translated into or out of the laser path. The ring electrode has been modified by drilling a 3.2 mm hole through the center, perpendicular to the axial direction. The laser beam is passed through the hole and out the opposite side of the ring electrode into a beam dump (the inside of a [1/2]-inch Cajon fitting painted black with Aerodag).

IRMPD fragmentation efficiency measurements are used to center the laser beam on the trapped ion cloud for maximum overlap, with and without the focusing lens. A peptide ion is trapped at a q_z of 0.40 to minimize the axial size of the ion cloud. The laser beam is translated axially until maximum dissociation is observed. The laser beam is translated to either side to confirm the position at the center of the ion cloud, as dissociation is reduced at equal distances from the center. The vertical position of the laser beam is also adjusted for maximum dissociation.

Results and Discussion

Laser Power and Overlap with the Ion Cloud

The beam waist of the unfocused and focused laser was measured at the focal length, outside the vacuum system. A razor blade on a precision translation stage was used to measure the beam waist by finding the positions where beam power was attenuated by 7% and 93%, defined as the beam diameter, and dividing the difference by $\sqrt{2}$ to relate the Gaussian beam profile to a full width at half maximum. The unfocused laser beam waist was measured nine times for an average of 3.63 ± 0.07 mm, but in IRMPD experiments the laser beam is clipped at the edge of the smaller, 3.2 mm hole in the ring electrode. The focused laser beam waist was also measured nine times at the focal point for an average of 0.94 ± 0.04 mm.

The axial amplitudes of trapped ion clouds at a q_z of 0.10 and helium bath gas pressure of 3.3×10^{-4} Torr, reduced from 1.0×10^{-3} Torr to prevent significant collisional cooling for IRMPD, were measured with laser tomography [20, 21] (Figure 1). The focused laser was axially translated away from the center of the trapping volume up to ~ 1 mm without clipping the edge of the hole in the ring electrode. Overlap with the ion cloud decreases as the focused laser beam is translated axially, and fragmentation efficiency decreases accordingly. The larger m/z ion had a smaller measured ion cloud at the same q_z , as predicted [22]. Ion cloud axial amplitudes have also been shown to decrease with increasing bath gas pressure [20]. The profile of $[\text{PD} + \text{H}]^+$ at 3.3×10^{-4} Torr and a q_z of 0.10 represents the largest ion cloud in these IRMPD experiments and is larger than the beam waist of the focused

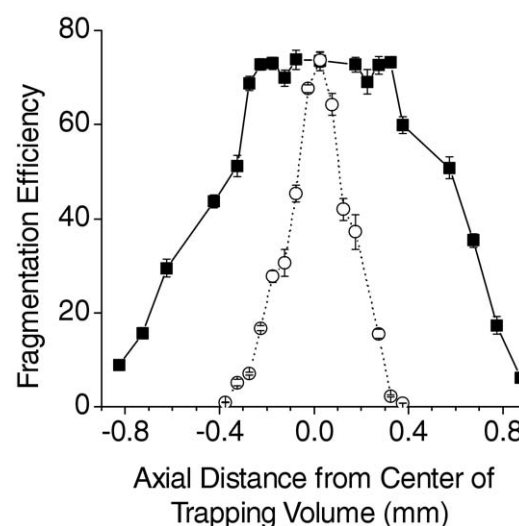


Figure 1. Laser tomography of $[\text{PD} + \text{H}]^+$ (filled square), m/z 231, and $[\text{melittin} + 4\text{H}]^{4+}$ (open circle), m/z 712, at a constant helium bath gas pressure of 3.3×10^{-4} Torr and a q_z of 0.10 (95% confidence error bars). Constant irradiation times of 7 ms for $[\text{PD} + \text{H}]^+$ and 1.75 ms for $[\text{melittin} + 4\text{H}]^{4+}$ were used to approximately match peak fragmentation efficiency.

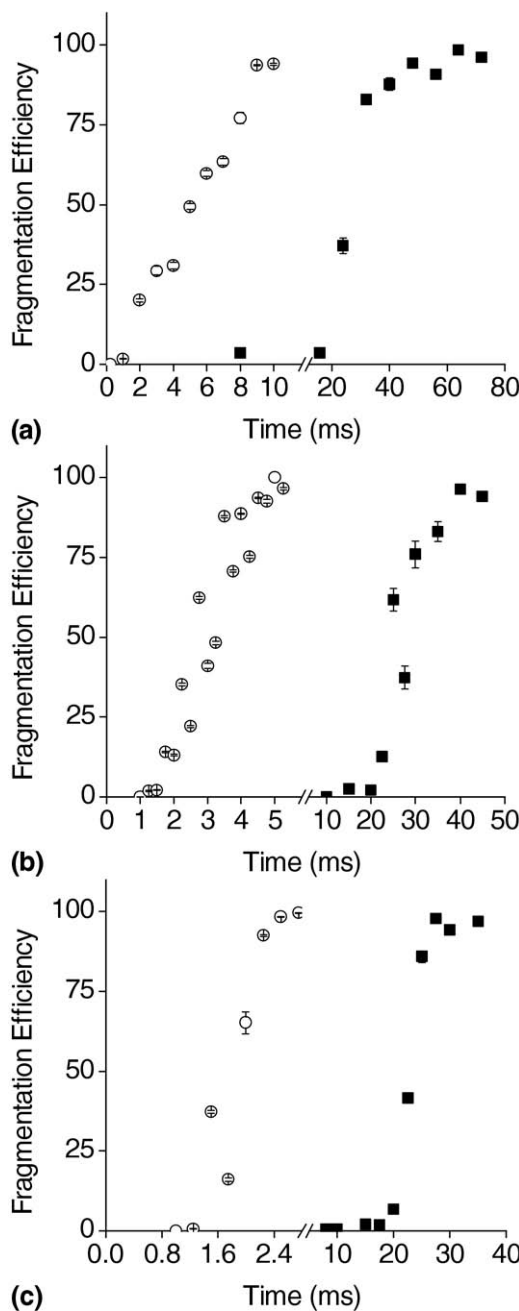


Figure 2. IRMPD at a constant helium bath gas pressure of 3.3×10^{-4} Torr with the laser unfocused (filled square) and focused (open circle) of (a) $[PD + H]^+$, m/z 231; (b) $[bradykinin + 2H]^{2+}$, m/z 531; and (c) $[melittin + 4H]^{4+}$, m/z 712 (95% confidence error bars).

laser. The unfocused laser irradiates an area up to three times larger than trapped ion clouds, and much of the radiation is not absorbed because the ion cloud does not overlap the whole beam spot. The focused laser beam is smaller than or similar in size to all trapped ion clouds, increasing the overlap of the ion cloud with the laser. Laser flux on the ion cloud is also increased by focusing laser intensity on a smaller area.

The laser beam power was measured at two positions: the center of the ring electrode and 30.5 cm

beyond the center of the ring electrode. Laser power at the center of the trap was measured external to the vacuum housing by passing the laser through a separate, 3.2 mm aperture equal to the hole in the ring electrode. The power of the unfocused laser was reduced by clipping at the edge of the hole in the ring electrode, and the power of the focused laser was 1.9 ± 0.3 times greater. Taking the focused beam waist and

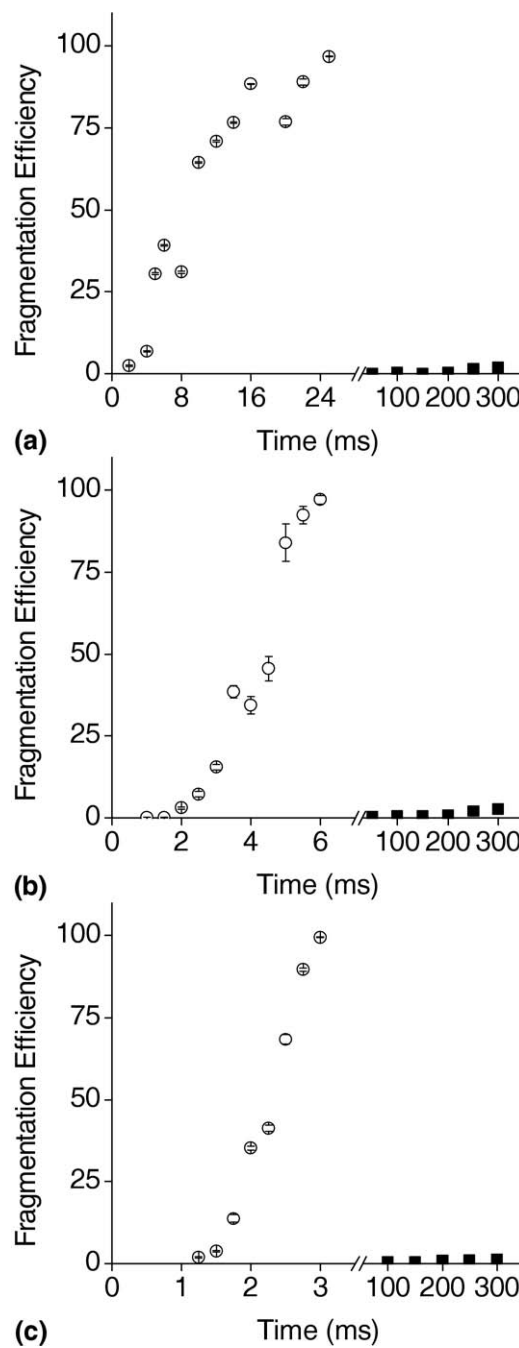


Figure 3. IRMPD at a constant helium bath gas pressure of 1.0×10^{-3} Torr with the laser unfocused (filled square) and focused (open circle) of (a) $[PD + H]^+$, m/z 231; (b) $[bradykinin + 2H]^{2+}$, m/z 531; and (c) $[melittin + 4H]^{4+}$, m/z 712 (95% confidence error bars).

Table 1. Product ion abundances from IRMPD of $[ALILTLVS + H]^+$ with the laser unfocused at helium bath gas pressure of 3.3×10^{-4} Torr

Irradiation time (ms)	% Fragmentation efficiency	% MS/MS efficiency	b_7^+ abundance	$[b_6\text{-H}_2\text{O}]^+$ abundance	b_5^+ abundance	b_4^+ abundance	b_3^+ abundance	b_2^+ abundance
25	28 ± 1	18.3 ± 0.8	12 ± 4	3.8 ± 0.8	0 ± 0	0 ± 0	0 ± 0	0 ± 0
30	63 ± 1	31.6 ± 0.8	$15 \pm 2^*$	$28 \pm 2^*$	$1.6 \pm 0.5^*$	$2.5 \pm 0.6^*$	0 ± 0	0 ± 0
40	88 ± 2	34 ± 1	2.3 ± 6	25 ± 2	0.4 ± 0.3	1.9 ± 0.5	0.8 ± 0.8	0 ± 0
45	95 ± 2	33.9 ± 0.9	1.5 ± 6	25 ± 1	0 ± 0	1.8 ± 0.5	0.7 ± 0.7	0 ± 0
50	99 ± 2	32.3 ± 0.9	0.3 ± 0.2	17.4 ± 0.9	0 ± 0	0.7 ± 0.3	0 ± 0	0.3 ± 0.2

*The largest abundance observed for each ion is shown in bold.

the hole in the ring electrode as diameters of a circular beam spot, respectively, the average flux of the focused laser per square millimeter is 6 ± 1 times greater than the average flux of the unfocused laser. Only the high-probability area of the ion cloud is irradiated by the focused laser spot instead of a larger area through the trapping volume.

IRMPD Efficiency

Increased laser flux on the ion cloud produces greater fragmentation efficiency and increases the dependence of fragmentation efficiency on ion cloud size. IRMPD of ions with the laser unfocused and focused was compared at a helium bath gas pressure of 3.3×10^{-4} Torr (Figure 2), reduced from 1.0×10^{-3} Torr to decrease collisional cooling. By using the focused laser, 7 to 12 times less irradiation time was required to achieve 100% fragmentation efficiency for respective parent ions compared to IRMPD with the unfocused laser. Fragmentation efficiency at a given irradiation time was also observed to increase with ion mass. Two factors explain the IRMPD mass dependence. Larger peptide ions with more residues have more IR-active groups, increasing absorption and dissociation despite having more degrees of freedom. Larger m/z ions also remain closer to the center of the trap and the most intense part of the laser. The focused laser increases the importance of the second factor because of the greater laser flux at the center of the trap.

IRMPD of ions with the laser unfocused and focused was also compared at a helium bath gas pressure of 1.0×10^{-3} Torr (Figure 3). Irradiation times for equivalent fragmentation efficiencies were increased compared to IRMPD at 3.3×10^{-4} Torr because of the

increased collisional cooling. No more than 3% fragmentation efficiency could be achieved for any ion after 300 ms irradiation with the unfocused laser. Less than 30 ms was required to achieve 100% fragmentation efficiency for all parent ions with the focused laser. This is 3 to 10 times less irradiation time for respective parent ions compared to IRMPD at 3.3×10^{-4} Torr with the unfocused laser. Irradiation time was not as short as IRMPD with a focused laser at 3.3×10^{-4} Torr, and smaller ions required a greater relative increase in irradiation time at 1.0×10^{-3} Torr. The rate of collisional cooling decreases with increasing mass [23], and the dissociation of larger ions is decreased less by collisional cooling at 1.0×10^{-3} Torr. Larger ions also have greater IR activity and are closer to the center of the laser.

A bath gas at 1.0×10^{-3} Torr improves detection over lower pressures, and efficient IRMPD at 1.0×10^{-3} Torr with the focused laser allows product ions to be observed in greater abundance. Table 1 shows efficiency values and product ion abundances from IRMPD of $[ALILTLVS + H]^+$ at 3.3×10^{-4} Torr with the unfocused laser. As fragmentation efficiency of the parent ion increased, product ion abundances grew to a maximum and then decreased due to sequential dissociation. MS/MS efficiency did not increase above 34% with increasing fragmentation efficiency because some product ions were sequentially dissociated to below the LMCO even at a q_z of 0.10. Product ion abundances from IRMPD of $[ALILTLVS + H]^+$ at 1.0×10^{-3} Torr with the focused laser are shown in Table 2 at similar fragmentation efficiencies to Table 1. Absolute product ion abundances were increased four to 40 times with IRMPD at the higher bath gas pressure and there was no change in the background noise. Several product

Table 2. Product ion abundances from IRMPD of $[ALILTLVS + H]^+$ with the laser focused at helium bath gas pressure of 1.0×10^{-3} Torr

Irradiation time (ms)	% Fragmentation efficiency	% MS/MS efficiency	b_7^+ abundance	$[b_6\text{-H}_2\text{O}]^+$ abundance	b_5^+ abundance	b_4^+ abundance	b_3^+ abundance	b_2^+ abundance
3	22.3 ± 0.7	19.6 ± 0.6	520 ± 40	23 ± 3	7 ± 1	1.5 ± 0.5	0.3 ± 0.3	0 ± 0
4	65 ± 2	38.6 ± 0.7	$570 \pm 30^*$	$124 \pm 9^*$	$29 \pm 2^*$	$19 \pm 2^*$	7 ± 2	0.3 ± 0.2
6	87 ± 2	42.6 ± 0.8	280 ± 20	88 ± 6	23 ± 2	15 ± 2	$26 \pm 3^*$	8 ± 1
8	96 ± 2	32.9 ± 0.4	55 ± 5	65 ± 5	7.8 ± 9	3.5 ± 0.8	22 ± 2	$14 \pm 2^*$
9	100 ± 2	22.4 ± 0.3	3 ± 1	25 ± 3	1.2 ± 0.8	0.6 ± 0.4	9 ± 2	13 ± 3

*The largest abundance observed for each ion is shown in bold.

ions, such as b_3^+ and b_2^+ , were only reliably observed at 1.0×10^{-3} Torr. MS/MS efficiency increased to a maximum of 43% and was lower at 100% fragmentation efficiency compared with MS/MS efficiency reported in Table 1. Sequential dissociation of product ions increases from the high flux of the focused laser, and more product ions are formed below the LMCO and not observed, decreasing MS/MS efficiency. Sequential dissociation is further increased for the reduced ion cloud sizes at 1.0×10^{-3} Torr, but the greater sensitivity at higher pressure increases observed product ion abundances despite more extensive sequential dissociation.

Conclusions

Sensitivity is increased and experiment time is decreased by performing IRMPD with a focused laser at 1.0×10^{-3} Torr. No modification to the standard IRMPD experiment is required, and the only instrumental modification consists of the simple addition of a lens to the laser optics. Higher sensitivity at 1.0×10^{-3} Torr allows product ions to be observed in greater abundance compared to the reduced pressures usually employed for IRMPD. Irradiation time is greatly reduced by focusing the laser beam to a spot similar to the axial amplitudes of trapped ion clouds at a q_z of 0.10. The laser flux on the ion cloud is increased six times by focusing laser power on the smaller area. IRMPD with the focused laser can dissociate larger peptide ions that have greater overlap with the high-flux laser and more IR-active groups. IRMPD of less easily dissociated ions might now be possible on a timescale no greater than previous experiments with an unfocused laser, such as <100 Da volatile organic compounds with few vibrational degrees of freedom, or $>m/z$ 2000 nanoparticles with many degrees of freedom and few IR-active groups.

Acknowledgments

The authors acknowledge support for this work by NSF grant CHE-0431825.

References

- Stephenson, J. L.; Booth, M. M.; Shalosky, J. A.; Eyler, J. R.; Yost, R. A. Infrared Multiple Photon Dissociation in the Quadrupole Ion Trap Via a Multipass Optical Arrangement. *J. Am. Soc. Mass Spectrom.* **1994**, *5*, 886–893.
- Colorado, A.; Shen, J. X.; Vartanian, V. H.; Brodbelt, J. Use of Infrared Multiphoton Photodissociation with Swift for Electrospray Ionization and Laser Desorption Applications in a Quadrupole Ion Trap Mass Spectrometer. *Anal. Chem.* **1996**, *68*, 4033–4043.
- Goolsby, B. J.; Brodbelt, J. S. Characterization of B-Lactams by Photodissociation and Collision-Activated Dissociation in a Quadrupole Ion Trap. *J. Mass Spectrom.* **1998**, *33*, 705–712.
- Payne, A. H.; Glish, G. L. Thermally Assisted Infrared Multiphoton Photodissociation in a Quadrupole Ion Trap. *Anal. Chem.* **2001**, *73*, 3542–3548.
- Shen, J.; Brodbelt, J. S. Characterization of Ionophore-Metal Complexes by Infrared Multiphoton Photodissociation and Collision-Activated Dissociation in a Quadrupole Ion Trap Mass Spectrometer. *Analyst* **2000**, *125*, 641–650.
- Crowe, M. C.; Brodbelt, J. S.; Goolsby, B. J.; Hergenrother, P. Characterization of Erythromycin Analogs by Collisional Activated Dissociation and Infrared Multiphoton Dissociation in a Quadrupole Ion Trap. *J. Am. Soc. Mass Spectrom.* **2002**, *13*, 630–649.
- Keller, K. M.; Brodbelt, J. S. Collisionally Activated Dissociation and Infrared Multiphoton Dissociation of Oligonucleotides in a Quadrupole Ion Trap. *Anal. Biochem.* **2004**, *326*, 200–210.
- Little, D. P.; Speir, J. P.; Senko, M. W.; O'Connor, P. B.; McLafferty, F. W. Infrared Multiphoton Dissociation of Large Multiply Charged Ions for Biomolecule Sequencing. *Anal. Chem.* **1994**, *66*, 2809–2815.
- Little, D. P.; Aaserud, D. J.; Valaskovic, G. A.; McLafferty, F. W. Sequence Information from 42–108-Mer DNAs (complete for a 50-Mer) by Tandem Mass Spectrometry. *J. Am. Soc. Mass Spectrom.* **1996**, *118*, 9352–9359.
- Xie, Y.; Lebrilla, C. B. Infrared Multiphoton Dissociation of Alkali Metal-Coordinated Oligosaccharides. *Anal. Chem.* **2003**, *75*, 1590–1598.
- Sleno, L.; Volmer, D. A. Ion Activation Methods for Tandem Mass Spectrometry. *J. Mass Spectrom.* **2004**, *39*, 1091–1112.
- Stafford, G. C. J.; Kelley, P. E.; Syka, J. E. P.; Reynolds, W. E.; Todd, J. F. J. Recent Improvements in and Analytical Applications of Advanced Ion Trap Technology. *Int. J. Mass Spectrom. Ion Processes* **1984**, *60*, 85–98.
- Black, D. M.; Payne, A. H.; Glish, G. L. Determination of Cooling Rates in a Quadrupole Ion Trap. *J. Am. Soc. Mass Spectrom.* **2006**, *17*, 932–938.
- Hashimoto, Y.; Hasegawa, H.; Yoshinari, K.; Waki, I. Collision-Activated Infrared Multiphoton Dissociation in a Quadrupole Ion Trap Mass Spectrometer. *Anal. Chem.* **2003**, *75*, 420–425.
- Boué, S. M.; Stephenson, J. L.; Yost, R. A. Pulsed Helium Introduction into Quadrupole Ion Trap for Reduced Collisional Quenching During Infrared Multiphoton Dissociation of Electrosprayed Ions. *Rapid Commun. Mass Spectrom.* **2000**, *14*, 1391–1397.
- Pikulski, M.; Wilson, J. J.; Aguilar, A.; Brodbelt, J. S. Amplification of Infrared Multiphoton Dissociation Efficiency in a Quadrupole Ion Trap Using Ir-Active Ligands. *Anal. Chem.* **2006**, *78*, 8512–8517.
- Pikulski, M.; Hargrove, A.; Shabbir, S. H.; Anslyn, E. V.; Brodbelt, J. S. Sequencing and Characterization of Oligosaccharides Using Infrared Multiphoton Dissociation and Boronic Acid Derivatization in a Quadrupole Ion Trap. *J. Am. Soc. Mass Spectrom.* **2007**, *18*, 2094–2106.
- Laskin, J.; Furtrell, J. H. Activation of Large Ions in FT-ICR Mass Spectrometry. *Mass Spectrom. Rev.* **2005**, *24*, 135–167.
- Yates, N.; Yost, R. 1992. ICMS Ion Trap Software. Release 2.20 unpublished, University of Florida, Gainesville, FL.
- Hemberger, P. H.; Nogar, N. S.; Williams, J. D.; Cooks, R. G.; Syka, J. E. P. Laser Photodissociation Probe for Ion Tomography Studies in a Quadrupole Ion-Trap Mass Spectrometer. *Chem. Phys. Lett.* **1992**, *191*, 405–410.
- Williams, J. D.; Cooks, R. G.; Syka, J. E. P.; Hemberger, P. H.; Nogar, N. S. Determination of Positions, Velocities, and Kinetic Energies of Resonantly Excited Ions in the Quadrupole Ion Trap Mass Spectrometer by Laser Photodissociation. *J. Am. Soc. Mass Spectrom.* **1993**, *4*, 792–797.
- Remes, P. M.; Glish, G. L. Mapping the Distribution of Ion Positions as a Function of Quadrupole Ion Trap Mass Spectrometer Operating Parameters to Optimize Infrared Multiphoton Dissociation. *J. Phys. Chem. A* **2009**, in press.
- Goeringer, D. E.; McLuckey, S. A. Relaxation of Internally Excited High-Mass Ions Simulated under Typical Quadrupole Ion Trap Storage Conditions. *Int. J. Mass Spectrom.* **1998**, *177*, 163–174.